Available online at http://scik.org
Commun. Math. Biol. Neurosci. 2022, 2022:111
https://doi.org/10.28919/cmbn/7735
ISSN: 2052-2541

DYNAMIC ANALYSIS OF A PREDATOR-PREY MODEL WITH HOLLING TYPE-II FUNCTIONAL RESPONSE AND PREY REFUGE BY USING A NSFD SCHEME

R. AHMED[1,*], J. MUSHTAQ[2], S. SAHER[2], H. M. A. SAEED[2]

[1]Department of Mathematics, Air University Multan Campus, Multan, Pakistan
[2]National College of Business Administration & Economics, Rahim Yar Khan, Pakistan

Abstract. This study proposes and analyzes a nonstandard finite difference (NSFD) scheme to retain the fundamental qualitative aspects of a predator-prey interaction with a Holling type-II functional response and prey refuge. The existence and stability of fixed points are examined. A few numerical examples are presented to back up the theoretical findings. The results show that the numerical simulations match well with the theoretical outcomes. Moreover, the model experiences transcritical, period-doubling, and Neimark-Sacker bifurcation. Furthermore, numerical simulations show that standard numerical methods like the Euler method and the classical RK4 method are not dynamically consistent with the continuous model. As a result, they do not accurately reflect the continuous model's behavior. The proposed NSFD scheme, on the other hand, is shown to be suitable and adequate for solving the continuous model.

Keywords: predator-prey; stability; bifurcation; non-standard finite difference.
2010 AMS Subject Classification: 39A28, 39A30.

1. INTRODUCTION

The predator and prey interaction is a complicated process in ecosystems owing to the nature of the relationship between the two. Many intrinsic and extrinsic factors may influence the

*Corresponding author
E-mail address: rizwanahmed488@gmail.com
Received September 13, 2022

dynamics of a population. Lotka [1], and Volterra [2] did the primarily accurate work on the predator-prey dynamical mathematical model. Since then, several predator-prey models have been developed to comprehend population dynamics and interactions. Numerous modifications of the Lotka-Volterra model have been presented and explored over the past half-century. An important component of these models is the so-called functional response, which represents the interaction between prey and predators. This functional reaction is significantly influenced by the behavior of the prey and the predator. In 1965, Holling [3] proposed three types of functional responses. Later, researchers such as Crowley-Martin [4] and Beddington-DeAngelis [5, 6] provided various functional responses. After that, many researchers looked at models that were developed on interactions between predators and prey, including various kinds of functional responses [7–10].

The Holling type II functional response occurs in animals when the amount of prey devoured grows fast along with the density of prey. This functional response is represented by $\frac{mx}{1+x}$, where the parameter m is the maximum predation rate per capita. The pair of equations below is a generic formulation of the predator-prey model with Holling type-II functional response:

$$
\begin{cases}
\frac{dx}{dt} = rx(1-\frac{x}{k}) - \frac{mxy}{1+x}, \\
\frac{dy}{dt} = \frac{cxy}{1+x} - by,
\end{cases}
\tag{1.1}
$$

where $x(t)$, $y(t)$ is the number of prey and predator at the time t, respectively. Here k is carrying capacity, r and c are growth rates of prey and predator, respectively, m is predation rate, and b is the natural death rate of the predator.

In evolutionary biology, the concept of prey refuge refers to how an organism can protect itself from being eaten by a predator by hiding in a location inaccessible to the predator. For instance, in a model involving wolves and ungulates, the ungulates may seek refuge by relocating to places outside of the wolves' core territory. Additionally, it plays several essential roles in the dynamics of interactions between predators and prey. For example, the presence of prey refuges might reduce the likelihood that animals would go extinct. Let ex represent the number of prey free from predation, and so $(1-e)x$ represents the number of prey that are vulnerable to being eaten by the predator. Thus, in the presence of a prey refuge, a modified variant of the Holling type-II functional response is given by

$$f(x) = \frac{m(1-e)x}{1+x},$$

where e is the prey refuge parameter and e lies in the interval $(0,1)$.

After incorporating the refuge effect, the model (1.1) becomes

$$\begin{cases} \frac{dx}{dt} = rx(1-\frac{x}{k}) - \frac{m(1-e)xy}{1+x}, \\ \frac{dy}{dt} = \frac{cxy}{1+(1-e)x} - by. \end{cases} \tag{1.2}$$

Harvesting is always one of the essential aspects in the dynamics of the predator-prey model, according to the demands of humans and long-term development, the exploitation of natural resources, and the storage of renewable energy [11]. We discover that the predator-prey model with harvesting may result in more complicated features than the one without harvesting [12–15], which motivates us to include harvesting. May [16] proposed two kinds of harvesting regimes: constant-yield harvesting (representing harvested biomass independent of population size) and constant-effort harvesting (representing harvested biomass proportional to the size of the population). Based on the model (1.2), we construct a constant-effort harvesting predator-prey model

$$\begin{cases} \frac{dx}{dt} = rx(1-\frac{x}{k}) - \frac{m(1-e)xy}{1+x} - a_1E_1x, \\ \frac{dy}{dt} = \frac{cxy}{1+(1-e)x} - by - a_2E_2y, \end{cases} \tag{1.3}$$

where a_1 and a_2 are catch coefficients of prey and predator, E_1 and E_2 are harvest rates of prey and predator.

For simplicity, we take $r_1 = r - a_1E_1$ and $r_2 = b + a_2E_2$. The model (1.3) reduces to

$$\begin{cases} \frac{dx}{dt} = r_1x - \frac{rx^2}{k} - \frac{m(1-e)xy}{1+x}, \\ \frac{dy}{dt} = \frac{cxy}{1+(1-e)x} - r_2y. \end{cases} \tag{1.4}$$

For a variety of reasons, discrete-time models are superior to continuous-time models. Because the exact analytical solutions of continuous-time models are unknown, discretization is required to produce discrete-time models that estimate the exact solutions. Model simulations also entail using digital computers, which necessitate the use of discrete-time models. To obtain the discrete predator-prey model, we employ a non-standard finite difference scheme (NSFDS) of Mickens-type [17] to discretize the model (1.4) as follows:

$$
\begin{cases} \frac{x_{n+1}-x_n}{h} = r_1 x_n - \frac{r x_n x_{n+1}}{k} - \frac{(1-e)m x_n y_n}{1+x_n}, \\ \frac{y_{n+1}-y_n}{h} = \frac{(1-e)c x_n y_n}{1+x_n} - r_2 y_n. \end{cases} \tag{1.5}
$$

After simple computations, the discrete counterpart of (1.4) obtained by the non-standard finite difference method is as follows:

$$
\begin{cases} x_{n+1} = \frac{r_1 x_n h k}{k+h r x_n} - \frac{hk(1-e)m x_n y_n}{(k+h r x_n)(1+x_n)} + \frac{k x_n}{k+h r x_n}, \\ y_{n+1} = \frac{h(1-e)c x_n y_n}{1+x_n} - h r_2 y_n + y_n. \end{cases} \tag{1.6}
$$

All parameters r_2, r, h, k, e, m, c are positive and $0 < e < 1$. The parameter r_1 can take positive or negative real values.

Our main results include an investigation of stability and bifurcation in the model and chaos control. We direct the readers' attention to [18–21] for a more in-depth consideration of stability, bifurcation, and chaos control.

The rest of the paper is organized as follows: Section (2) discusses the existence of equilibria and their topological categorization. To illustrate the theoretical research, numerical examples for model(1.6) are provided in section (3). The section (3) also contains a comparison of the NSFD scheme to the SFD scheme. Finally, in section (4), a concise conclusion is given.

2. Existence and Topological Classification of Fixed Points

To determine the fixed points $(\bar{x}, \bar{y})$ of the model (1.6), we solve the following system of equations:

$$
\begin{cases} \bar{x} = \frac{r_1 \bar{x} h k}{k+h r \bar{x}} - \frac{hk(1-e)m \bar{x}\bar{y}}{(k+h r \bar{x})(1+\bar{x})} + \frac{k\bar{x}}{k+h r \bar{x}}, \\ \bar{y} = \frac{h(1-e)c\bar{x}\bar{y}}{1+\bar{x}} - h r_2 \bar{y} + \bar{y}. \end{cases} \tag{2.1}
$$

By simple computations, we obtain the following three fixed points of the model (1.6):

$$
E_0(0,0),\ E_1(\frac{r_1 k}{r},0),\ E_2\left(\frac{r_2}{(1-e)c-r_2}, -\frac{c(c(-1+e)kr_1+(r+kr_1)r_2)}{km(c(-1+e)+r_2)^2}\right).
$$

For the existence of E_1 we require the condition $r_1 > 0$.

Clearly, $\frac{r_2}{(1-e)c-r_2} > 0$ iff

$$r_2 < c(1-e).$$

Next, we solve the inequality

$$-\frac{c(c(-1+e)kr_1 + (r+kr_1)r_2)}{km(c(-1+e)+r_2)^2} > 0.$$

It implies that

$$c(-1+e)kr_1 + (r+kr_1)r_2 < 0. \tag{2.2}$$

From (2.2), it is observed that

$$kr_1((c(1-e)-r_2) > rr_2.$$

Since $r_2 < c(1-e)$, the above inequality has a solution only if $r_1 > 0$.

From (2.2), we can write

$$r_2 < \frac{ckr_1(1-e)}{r+kr_1}. \tag{2.3}$$

Since $r_2 > 0$, therefore $\frac{ckr_1(1-e)}{r+kr_1}$ must be a positive number, otherwise the above inequality (2.3) do not have any solution.

Now as

$$\frac{ckr_1(1-e)}{r+kr_1} = c(1-e)(1-\frac{r}{r+kr_1}) < c(1-e),$$

therefore, $r_2 < \frac{ckr_1(1-e)}{r+kr_1}$ implies that $r_2 < c(1-e)$. From these observations, we conclude that

$$E_2\left(\frac{r_2}{(1-e)c-r_2}, -\frac{c(c(-1+e)kr_1+(r+kr_1)r_2)}{km(c(-1+e)+r_2)^2}\right)$$

is the only positive fixed point of the model (1.6) iff $r_1 > 0$ and

$$0 < r_2 < \frac{ckr_1(1-e)}{r+kr_1}.$$

The Jacobian matrix J of the model computed at $(\bar{x},\bar{y})$ is given by

$$J(\bar{x},\bar{y}) = \begin{bmatrix} j_{11} & j_{12} \\ j_{21} & j_{22} \end{bmatrix},$$

where

$$j_{11} = \frac{k(-(-1+e)h^2mr\bar{x}^2\bar{y} + k((1+\bar{x})^2 + hr_1(1+\bar{x})^2 + (-1+e)hm\bar{y}))}{(1+\bar{x})^2(k+hr\bar{x})^2},$$

$$j_{12} = \frac{(-1+e)hkm\bar{x}}{(1+\bar{x})(k+hr\bar{x})},\ j_{21} = -\frac{c(-1+e)h\bar{y}}{(1+\bar{x})^2},\ j_{22} = 1 - hr_2 - \frac{ch(-1+e)\bar{x}}{1+\bar{x}}.$$

We use the following results to determine the local stability of fixed points in the model (1.6).

Lemma 2.1. *[22] Let $F(s) = s^2 + Ms + N$ be the characteristic equation of the Jacobian matrix $J((\bar{x},\bar{y}))$ and s_1, s_2 are two roots of $F(s) = 0$, then $(\bar{x},\bar{y})$ is*

(i) sink iff $|s_1| < 1$ and $|s_2| < 1$,

(ii) source iff $|s_1| > 1$ and $|s_2| > 1$,

(iii) saddle point iff $|s_1| < 1$ and $|s_2| > 1$ (or $|s_1| > 1$ and $|s_2| < 1$),

(iv) non-hyperbolic point iff either $|s_1| = 1$ or $|s_2| = 1$.

Lemma 2.2. *[22] Let $F(s) = s^2 + Ms + N$. Assume that $F(1) > 0$. If s_1, s_2 are two roots of $F(s) = 0$, then*

(i) $|s_1| < 1$ and $|s_2| < 1$ iff $F(-1) > 0$ and $N < 1$,

(ii) $|s_1| < 1$ and $|s_2| > 1$ (or $|s_1| > 1$ and $|s_2| < 1$) iff $F(-1) < 0$,

(iii) $|s_1| > 1$ and $|s_2| > 1$ iff $F(-1) > 0$ and $N > 1$,

(iv) $s_1 = -1$ and $|s_2| \neq 1$ iff $F(-1) = 0$ and $M \neq 0, 2$,

(v) s_1 and s_2 are complex and $|s_{1,2}| = 1$ iff $M^2 - 4N < 0$ and $N = 1$.

2.1. Topological Classification of $E_0(0,0)$.

We consider the following set:

$$\Gamma_0 = \left\{ (r_1, r_2, r, h, k, e, m, c) \in \mathbb{R}^8 : \text{all parameters are positive other than } r_1, \text{ and } 0 < e < 1 \right\}.$$

By using the lemma (2.1), we obtain the following result:

Lemma 2.3. *In the domain Γ_0, the fixed point $E_0(0,0)$ of the model* (1.6) *is*

(i) a sink iff $0 < r_2 < \frac{2}{h}$ and $-\frac{2}{h} < r_1 < 0$,

(ii) saddle point iff one of the following conditions holds

(a) $0 < r_2 < \frac{2}{h}$ and $r_1 > 0$,

or

(b) $0 < r_2 < \frac{2}{h}$ and $r_1 < -\frac{2}{h}$,

or

(c) $r_2 > \frac{2}{h}$ and $-\frac{2}{h} < r_1 < 0$,

(iii) source iff one of the following conditions holds

(a) $r_1 > 0$ and $r_2 > \frac{2}{h}$,

or

(b) $r_1 < -\frac{2}{h}$ and $r_2 > \frac{2}{h}$,

(iv) non-hyperbolic point iff one of the following conditions holds

(a) $r_1 = 0$,

or

(b) $r_1 < 0$ and $r_1 = -\frac{2}{h}$,

or

(c) $r_2 = \frac{2}{h}$.

Proof. The Jacobian matrix at $E_0(0,0)$ is given by

$$J(E_0) = \begin{bmatrix} 1+r_1h & 0 \\ 0 & 1-r_2h \end{bmatrix}. \tag{2.4}$$

The eigenvalues of $J(E_0)$ are $\lambda_1 = 1+r_1h$ and $\lambda_2 = 1-r_2h$. □

2.2. Topological Classification of $E_1(\frac{r_1k}{r},0)$.

We consider the following set:

$$\Gamma_1 = \left\{(r_1,r_2,r,h,k,e,m,c) \in \mathbb{R}^8 : \text{all parameters are positive and } 0<e<1\right\}.$$

By using the lemma (2.1), we obtain the following result:

Lemma 2.4. *In the domain Γ_1, the fixed point $E_1(\frac{r_1k}{r},0)$ of the model* (1.6) *is*

(i) a sink iff

$$\frac{c(1-e)kr_1}{r+kr_1} < r_2 < \frac{2}{h} + \frac{c(1-e)kr_1}{r+kr_1},$$

(ii) saddle point iff one of the following conditions holds

(a) $r_2 < \frac{c(1-e)kr_1}{r+kr_1}$,

or

(b) $r_2 > \frac{2}{h} + \frac{c(1-e)kr_1}{r+kr_1}$,

(iv) non-hyperbolic point iff one of the following conditions holds

(a) $r_2 = \frac{c(1-e)kr_1}{r+kr_1}$,

or

(b) $r_2 = \frac{2}{h} + \frac{c(1-e)kr_1}{r+kr_1}$.

Proof. The Jacobian matrix at $E_1(\frac{r_1k}{r},0)$ is given by

$$J(E_1) = \begin{bmatrix} \frac{1}{1+r_1h} & \frac{(-1+e)hkmr_1}{(1+hr_1)(r+kr_1)} \\ 0 & 1-r_2h-\frac{c(-1+e)hkr1}{r+kr_1} \end{bmatrix}. \tag{2.5}$$

The eigenvalues of $J(E_1)$ are $\lambda_1 = \frac{1}{1+r_1 h}$ and $\lambda_2 = 1 - r_2 h - \frac{c(-1+e)hkr1}{r+kr_1}$.

□

2.3. Topological Classification of $E_2\left(\frac{r_2}{(1-e)c-r_2}, -\frac{c(c(-1+e)kr_1+(r+kr_1)r_2)}{km(c(-1+e)+r_2)^2}\right)$.

We consider the following set:

$$\Gamma_2 = \Big\{(r_1, r_2, r, h, k, e, m, c) \in \mathbb{R}^8 : \text{all parameters are positive and}$$
$$0 < e < 1,\ 0 < r_2 < \frac{ckr_1(1-e)}{r+kr_1}\Big\}.$$

By using the lemma (2.1) and lemma (2.2), we obtain the following result:

Lemma 2.5. *In the domain Γ_2, the fixed point $E_2\left(\frac{r_2}{(1-e)c-r_2}, -\frac{c(c(-1+e)kr_1+(r+kr_1)r_2)}{km(c(-1+e)+r_2)^2}\right)$ of the model* (1.6) *is*

(i) a sink iff

$$k < \frac{r(r_2 - hr_2^2 - c(-1+e)(1+hr_2))}{r_1(c(-1+e)+r_2)(-1+c(-1+e)h+r_2 h)},$$

(ii) source iff

$$k > \frac{r(r_2 - hr_2^2 - c(-1+e)(1+hr_2))}{r_1(c(-1+e)+r_2)(-1+c(-1+e)h+r_2 h)},$$

(iv) non-hyperbolic point iff

$$k = \frac{r(r_2 - hr_2^2 - c(-1+e)(1+hr_2))}{r_1(c(-1+e)+r_2)(-1+c(-1+e)h+r_2 h)}.$$

Proof. The Jacobian matrix at the fixed point

$$E_2\left(\frac{r_2}{(1-e)c-r_2}, -\frac{c(c(-1+e)kr_1+(r+kr_1)r_2)}{km(c(-1+e)+r_2)^2}\right)$$

is given by

$$J(E_2) = \begin{bmatrix} J_{11} & J_{12} \\ J_{21} & 1 \end{bmatrix}, \tag{2.6}$$

where

$$J_{11} = \frac{c^2(-1+e)^2k - c(-1+e)k(-1+hr_1)r_2 - h(r+kr_1)r_2^2}{c(-1+e)(c(-1+e)k+(k-hr)r_2)},$$

$$J_{12} = -\frac{hkmr_2(c(-1+e)+r_2)}{c(c(-1+e)k+(k-hr)r_2)},\ J_{21} = \frac{h(cr_1 + \frac{(r+kr_1)r_2}{k(-1+e)})}{m}.$$

The characteristic polynomial of $J(E_2)$ is given by

$$F(s) = s^2 + Ms + N, \tag{2.7}$$

where

$$M = -\frac{(c(-1+e)+r_2)(2c(-1+e)k - h(r+kr_1)r_2)}{c(-1+e)(c(-1+e)k+(k-hr)r_2)},$$

and

$$N = \left(h(r+kr_1)r_2^2(-1+hr_2) + c^2(-1+e)^2k(1+h^2r_1r_2) + c(-1+e)r_2(k - hkr_1 + h^2rr_2 + 2h^2kr_1r_2)\right)\Big/\left(c(-1+e)(c(-1+e)k+(k-hr)r_2)\right).$$

Through simple computations, we obtain

$$F(1) = \frac{h^2r_2(c(-1+e)+r_2)(c(-1+e)kr_1 + (r+kr_1)r_2)}{c(-1+e)(c(-1+e)k+(k-hr)r_2)},$$

$$F(-1) = \frac{(c(-1+e)+r_2)(h(r+kr_1)r_2(-2+hr_2) + c(-1+e)k(4+h^2r_1r_2))}{c(-1+e)(c(-1+e)k+(k-hr)r_2)},$$

and

$$F(0) = \left(h(r+kr_1)r_2^2(-1+hr_2) + c^2(-1+e)^2k(1+h^2r_1r_2) + c(-1+e)r_2(k - hkr_1 + h^2rr_2 + 2h^2kr_1r_2)\right)\Big/\left(c(-1+e)(c(-1+e)k+(k-hr)r_2)\right).$$

We can write $F(1)$ as follows:

$$F(1) = \frac{h^2r_2(c(-1+e)+r_2)(c(-1+e)kr_1 + (r+kr_1)r_2)}{c(1-e)(c(1-e)k+(hr-k)r_2)}.$$

In Γ_2, since $c(1-e) > r_2$, therefore we have $c(-1+e)+r_2 < 0$. Moreover, as $ckr_1(1-e) > r_2(r+kr_1)$ in Γ_2, we have

$$\begin{aligned}
&-c(-1+e)kr_1+(r+kr_1)r_2\\
&=-c(1-e)kr_1+(r+kr_1)r_2\\
&<-c(1-e)kr_1+ckr_1(1-e)\\
&=-2ckr_1(1-e)<0.
\end{aligned}$$

It means that in Γ_2, we have

$$h^2r_2(c(-1+e)+r_2(c(-1+e)kr_1+(r+kr_1)r_2)>0. \tag{2.8}$$

Since $c(1-e) > r_2$, therefore, we have

$$\begin{aligned}
&c(1-e)k+(hr-k)r_2\\
&>r_2k+(hr-k)r_2\\
&=hrr_2>0.
\end{aligned}$$

It means that in Γ_2, we have

$$c(1-e)(c(1-e)k+(hr-k)r_2)>0. \tag{2.9}$$

Combining (2.8) and (2.9), we conclude that $F(1) > 0$ in Γ_2.

Since $r_2(r+kr_1) < ckr_1(1-e)$, we can write

$$\begin{aligned}
&h(r+kr_1)r_2(-2+hr_2+c(-1+e)k(4+h^2r_1r_2)\\
&=-2r_2h(r+kr_1)+r_2^2h^2(r+kr_1)-ck(1-e)(4+h^2r_1r_2)\\
&<-2r_2h(r+kr_1)+r_2h^2ckr_1(1-e)-ck(1-e)(4+h^2r_1r_2)\\
&=-2r_2h(r+kr_1)+ck(1-e)(r_1r_2h^2-4-h^2r_1r_2)\\
&=-2r_2h(r+kr_1)-4ck(1-e)<0.
\end{aligned}$$

Since we have $c(-1+e)+r_2 < 0$, therefore we have $F(-1) > 0$ in Γ_2.

After simple computations, we obtain that $F(0) = 1$ implies that

$$k = \frac{r(r_2 - hr_2^2 - c(-1+e)(1+hr_2))}{r_1(c(-1+e)+r_2)(-1+c(-1+e)h+r_2h)},$$

$F(0) > 1$ implies that

$$k > \frac{r(r_2 - hr_2^2 - c(-1+e)(1+hr_2))}{r_1(c(-1+e)+r_2)(-1+c(-1+e)h+r_2h)},$$

and $F(0) < 1$ implies that

$$k < \frac{r(r_2 - hr_2^2 - c(-1+e)(1+hr_2))}{r_1(c(-1+e)+r_2)(-1+c(-1+e)h+r_2h)}.$$

□

3. Numerical Simulations

This part provides numerical examples to validate our earlier theoretical results about the model's many qualitative features.

3.1. Stability analysis and Bifurcation of the model (1.6) at E_3 by using k as bifurcation parameter:

For model (1.6), we set the parameters and initial conditions as follows:

$r_1 = 0.5,\ r_2 = 0.1,\ r = 0.7,\ e = 0.3,\ c = 0.5,\ m = 0.7,\ h = 0.9,\ x_0 = 0.5,\ y_0 = 0.9.$

The bifurcation diagrams (1a,1b) of figure (1) depict that the model experiences Neimark-Sacker bifurcation for $k \gtrapprox 2.16$. The phase portrait depicted in figure (1c) shows that fixed point $E_2 \approx (0.4, 1.02857)$ is stable for $k = 2.14$. The phase portrait depicted in figure (1d) shows that the fixed point is unstable due to Neimark-Sacker bifurcation for $a = 2.17$.

3.2. Stability analysis and Bifurcation of the model (1.6) at E_3 by using e as bifurcation parameter:

For model (1.6), we set the parameters and initial conditions as follows:

$r_1 = 0.5,\ r_2 = 0.1,\ r = 0.7,\ h = 0.9,\ c = 0.5,\ m = 0.7,\ k = 2.15,\ x_0 = 0.5,\ y_0 = 0.9.$

The bifurcation diagrams (2a,2b) of figure (2) depict that model experiences transcritical bifurcation for $e \approx 0.669767$. One can check by using Jury test that for $e = 0.65$, the fixed point E_1 is unstable and fixed point E_2 is stable. Moreover, for $e = 0.65$, the fixed point E_1 is stable and fixed point E_2 is unstable. For $e \approx 0.669767$, the fixed points E_1 and E_2 collide and exchange their stability. It confirms the existence of transcritical bifurcation for $e \approx 0.669767$.

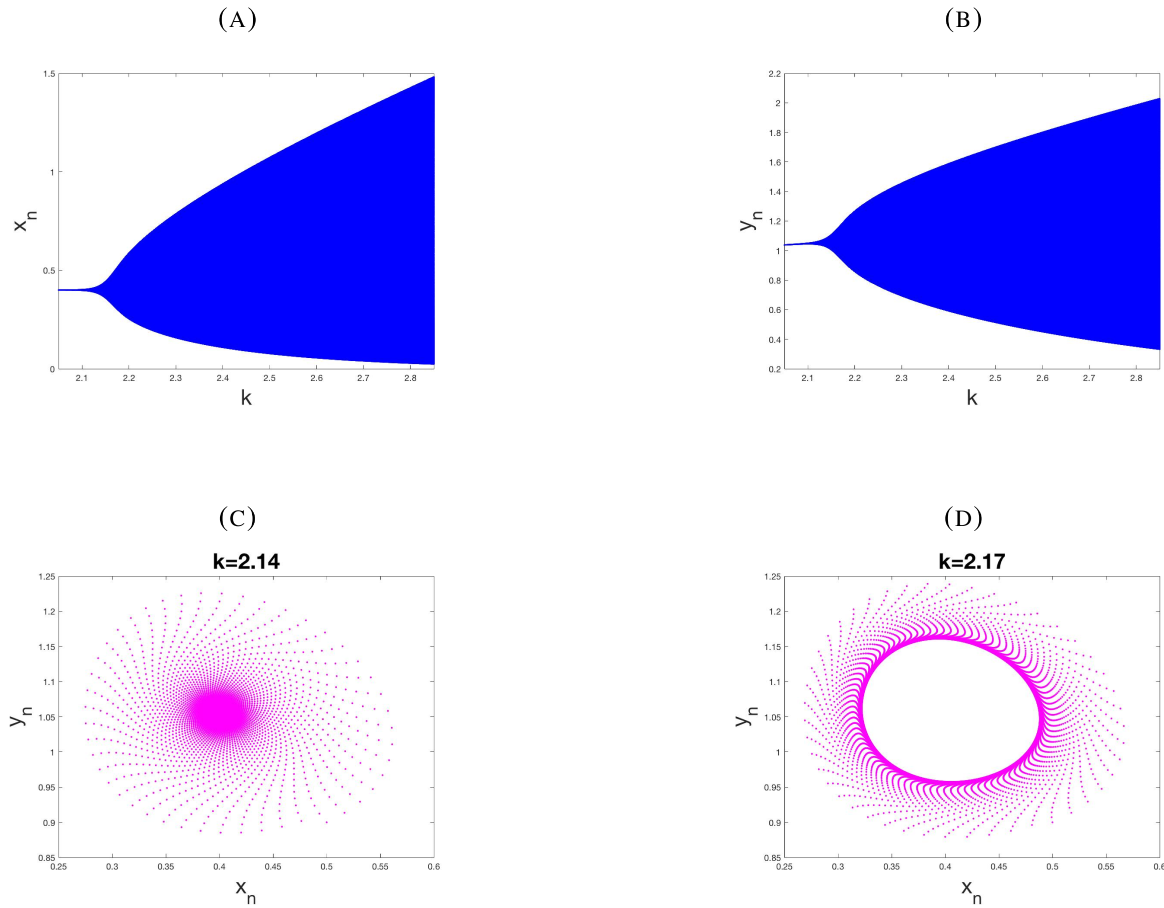

FIGURE 1. Bifurcation diagrams of (1.6) for $r_1 = 0.5,\ r_2 = 0.1,\ r = 0.7,\ e = 0.3,\ c = 0.5,\ m = 0.7,\ h = 0.9,\ x_0 = 0.5,\ y_0 = 0.9, k \in (2.05, 2.85)$, and phase portraits of model (1.6) for $k = 2.14$ and $k = 2.17$.

The bifurcation diagrams (2a,2b) of figure (2) depict that model experiences Neimark-Sacker bifurcation for $e \lessapprox 0.29616$.

(A) (B)

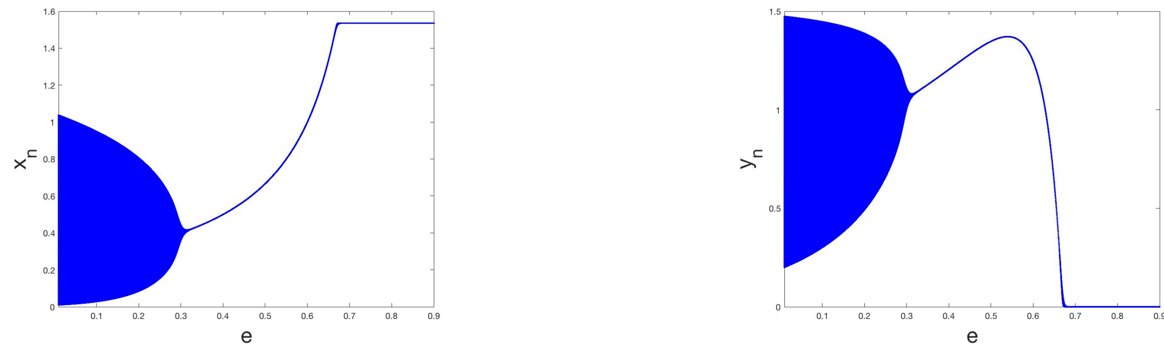

FIGURE 2. Bifurcation diagrams of (1.6) for $r_1 = 0.5,\ r_2 = 0.1,\ r = 0.7,\ h = 0.9,\ c = 0.5,\ m = 0.7,\ k = 2.15,\ x_0 = 0.5,\ y_0 = 0.9, e \in (0.01, 0.9)$.

We observe that the model (1.6) is stable for small values of carrying capacity k and unstable for large values of carrying capacity k. But, small values of prey refuge e destabilize the model, whereas large values of prey refuge e stabilize the model.

A similar investigation for other parameters r_1, r_2, r, h, c, m can be done by taking one as a bifurcation parameter and fixing all other parameters. All parameters affect the stability of the fixed point E_2 of the model (1.6).

3.3. Comparison of NSFD Scheme with SFD Schemes.

By using the forward Euler method, the discrete counterpart of (1.4) is given by

$$\begin{cases} x_{n+1} = x_n + h(r_1 x_n - \frac{r x_n^2}{k} - \frac{m(1-e)x_n y_n}{1+x_n}), \\ y_{n+1} = y_n + h(\frac{c x_n y_n}{1+(1-e)x_n} - r_2 y_n). \end{cases} \tag{3.1}$$

By applying the RK4 method to (1.4), we obtain the following discrete counterpart of (1.4):

$$x_{n+1} = x_n + \frac{1}{6}(K_1 + 2K_2 + 2K_3 + K_4),$$

$$y_{n+1} = y_n + \frac{1}{6}(L_1 + 2L_2 + 2L_3 + L_4),$$

$$K_1 = hf(x_n, y_n),\ L_1 = hg(x_n, y_n),$$

$$K_2 = hf(x_n + \frac{K_1}{2}, y_n + \frac{L_1}{2}),\ L_2 = hg(x_n + \frac{K_1}{2}, y_n + \frac{L_1}{2}),$$

$$K_3 = hf(x_n + \frac{K_2}{2}, y_n + \frac{L_2}{2}),\ L_3 = hg(x_n + \frac{K_2}{2}, y_n + \frac{L_2}{2}),$$
$$K_4 = hf(x_n + K_3, y_n + L_3),\ L_4 = hg(x_n + K_3, y_n + L_3),$$

where

$$f(x_n, y_n) = r_1 x_n - \frac{r x_n^2}{k} - \frac{m(1-e)x_n y_n}{1+x_n},$$

and

$$g(x_n, y_n) = \frac{c x_n y_n}{1+(1-e)x_n} - r_2 y_n.$$

By using a nonstandard finite difference(NSFD) scheme, we obtain the following discrete counterpart of (1.4):

$$\begin{cases} x_{n+1} = \frac{r_1 x_n hk}{k+hrx_n} - \frac{hk(1-e)m x_n y_n}{(k+hrx_n)(1+x_n)} + \frac{k x_n}{k+hrx_n}, \\ y_{n+1} = \frac{h(1-e)c x_n y_n}{1+x_n} - hr_2 y_n + y_n. \end{cases} \tag{3.2}$$

We set the parameters and initial conditions as follows:

$r_1 = 0.5,\ r_2 = 0.1,\ r = 0.7,\ e = 0.65,\ c = 0.5,\ m = 0.7,\ k = 2.15,\ x_0 = 0.5,\ y_0 = 0.9.$

Figure (3) depicts the numerical solutions produced by these numerical schemes. The numerical solutions produced by the Euler method are shown in figures (3a,3b) of figure (3), numerical solutions produced by the RK4 method are shown in figures (3c,3d) of figure (3), and numerical solutions produced by the NSFD method are shown in figures (3e,3f) of figure (3). The numerical solutions produced by the Euler technique and the RK4 approach reveal that the continuous model's boundedness and stability features are lost. The Euler and RK4 methods give numerical solutions oscillating near the fixed point. Meanwhile, the numerical solutions obtained by the NSFD scheme (1.6) converge to the fixed point. The fixed point is stable in the case of the NSFD scheme.

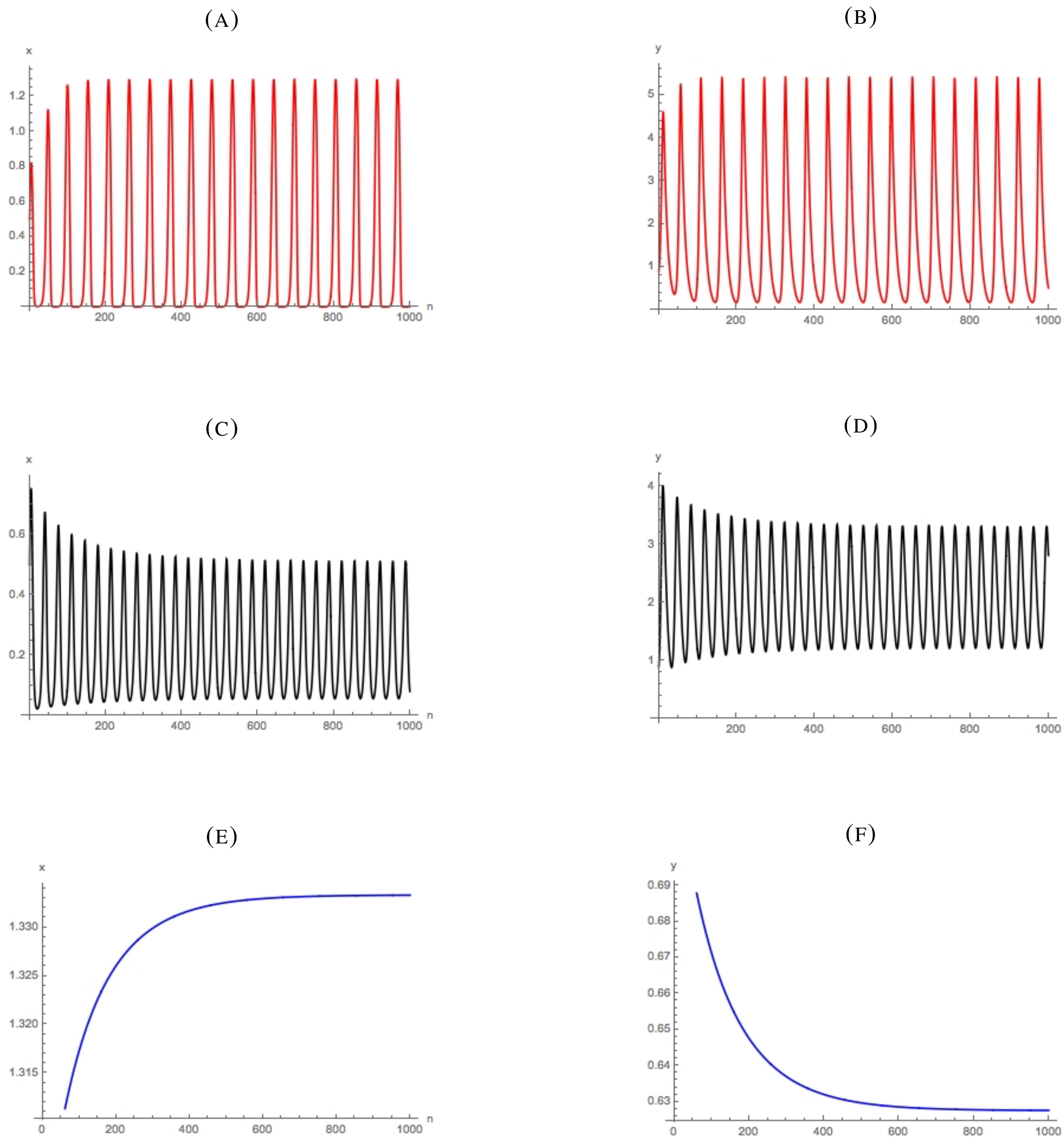

FIGURE 3. Time series graphs of x_n and y_n of system (1.4) by using the Euler method, the RK4 method, and the NSFD method for $r_1 = 0.5,\ r_2 = 0.1,\ r = 0.7,\ e = 0.65,\ c = 0.5,\ m = 0.7,\ k = 2.15,\ x_0 = 0.5,\ y_0 = 0.9$.

4. CONCLUSION

In this work, we studied a predator-prey model with Holling type-II functional response and prey refuge effect. We discretize the continuous model by using a non-standard finite difference scheme. The discrete model has three fixed points: two boundary points and one interior point. We examine the model's existence and stability conditions of fixed points by using the Jacobian matrix's eigenvalues and the Jury test. Moreover, it is shown that the model experiences three different types of bifurcations: transcritical, period-doubling, and Neimark-Sacker bifurcation. The numerical examples show the importance of prey refuge in the dynamics of the model. The small values of prey refuge e destabilize the model, whereas the large values of prey refuge e stabilize the model. A comparison of standard and non-standard finite difference methods is presented. It has been noted that the numerical solutions provided by the Euler technique and the RK4 approach reveal that the boundedness and stability features of the continuous model have been lost. The numerical solutions oscillate near the fixed point when using the Euler technique or the RK4 method. Meanwhile, the numerical solution obtained by the NSFD scheme (1.6) converges to the fixed point. The fixed point is stable in the case of the NSFD scheme.

CONFLICT OF INTERESTS

The authors declare that there is no conflict of interests.

REFERENCES

[1] A.J. Lotka, Elements of physical biology, Baltimore, Williams and Wilkins, (1925).

[2] V. Volterra, Variazioni e fluttuazioni del numero d'individui in specie animali conviventi. Memorie della Reale Accademia Nazionale dei Lincei Serie 6, 2 (1926), 31–113.

[3] C.S. Holling, Some characteristics of simple types of predation and parasitism, Can. Entomol. 91 (1959), 385–398. https://doi.org/10.4039/ent91385-7.

[4] P. Crowley, E.K. Martin, Functional responses and interference within and between year classes of a dragonfly population, J. North Amer. Benthol. Soc. 8 (1989), 211-221. https://www.jstor.org/stable/1467324.

[5] J.R. Beddington, Mutual interference between parasites or predators and its effect on searching efficiency, J. Animal Ecol. 44 (1975), 331-340. https://doi.org/10.2307/3866.

[6] D.L. DeAngelis, R.A. Goldstein, R.V. O'Neill, A model for tropic interaction, Ecology. 56 (1975), 881–892. https://doi.org/10.2307/1936298.

[7] M.F. Elettreby, A. Khawagi, T. Nabil, Dynamics of a discrete prey–predator model with mixed functional response, Int. J. Bifurcation Chaos. 29 (2019), 1950199. https://doi.org/10.1142/s0218127419501992.

[8] S.M.S. Rana, U. Kulsum, Bifurcation analysis and chaos control in a discrete-time predator-prey system of leslie type with simplified Holling type IV functional response, Discr. Dyn. Nat. Soc. 2017 (2017), 9705985. https://doi.org/10.1155/2017/9705985.

[9] S.M.S. Rana, Chaotic dynamics and control in a discrete-time predator-prey system with Ivlev functional response, Network Biol. 10 (2020), 45-61.

[10] S.M.S. Rana, Dynamic complexity in a discrete-time predator-prey system with Michaelis-Menten functional response: Gompertz growth of prey, Comput. Ecol. Software, 10 (2020), 117-132.

[11] J. Chen, J. Huang, S. Ruan, et al. Bifurcations of invariant tori in predator-prey models with seasonal prey harvesting, SIAM J. Appl. Math. 73 (2013), 1876–1905. https://doi.org/10.1137/120895858.

[12] S. Chakraborty, S. Pal, N. Bairagi, Predator–prey interaction with harvesting: Mathematical study with biological ramifications, Appl. Math. Model. 36 (2012), 4044–4059. https://doi.org/10.1016/j.apm.2011.11.029.

[13] X. Zhang, H. Zhao, Global stability of a diffusive predator–prey model with discontinuous harvesting policy, Appl. Math. Lett. 109 (2020), 106539. https://doi.org/10.1016/j.aml.2020.106539.

[14] M. Sen, P.D.N. Srinivasu, M. Banerjee, Global dynamics of an additional food provided predator–prey system with constant harvest in predators, Appl. Math. Comput. 250 (2015), 193–211. https://doi.org/10.1016/j.amc.2014.10.085.

[15] R. Ahmed, Complex dynamics of a fractional-order predator-prey interaction with harvesting, Open J. Discret. Appl. Math. 3 (2020), 24–32. https://doi.org/10.30538/psrp-odam2020.0040.

[16] R.M. May, J.R. Beddington, C.W. Clark, et al. Management of multispecies fisheries, Science. 205 (1979), 267–277. https://doi.org/10.1126/science.205.4403.267.

[17] R. E. Mickens, Nonstandard finite difference methods of differential equations, World Scientific, Singapore, (1994).

[18] Y.A. Kuznetsov, Elements of applied bifurcation theory, Springer, New York, 2004. https://doi.org/10.1007/978-1-4757-3978-7.

[19] S. Wiggins, Introduction to applied nonlinear dynamical systems and chaos, Springer, New York, 2003. https://doi.org/10.1007/b97481.

[20] R. Ahmed, M.S. Yazdani, Complex dynamics of a discrete-time model with prey refuge and Holling type-II functional response, J. Math. Comput. Sci. 12 (2022), 113. https://doi.org/10.28919/jmcs/7205.

[21] S. Akhtar, R. Ahmed, M. Batool, et al. Stability, bifurcation and chaos control of a discretized Leslie prey-predator model, Chaos Solitons Fractals. 152 (2021), 111345. https://doi.org/10.1016/j.chaos.2021.111345.

[22] A.C.J. Luo, Regularity and complexity in dynamical systems, Springer, New York, 2012. https://doi.org/10.1007/978-1-4614-1524-4.